# Modeling the Interphase of Silicone/$SiO_2$ Nanodielectrics

M. Paredes, C. Angammana, and S. Jayaram
Department of Electrical & Computer Engineering
University of Waterloo
Waterloo, ON N2L3G1, Canada

## ABSTRACT

The incorporation of inorganic nanoparticles in a polymer matrix enhances the dielectric performance. The improved properties, which the nanocomposites exhibit, are due to the behavior of the interfacial interaction zone which surrounds the nanoparticles. Because of the high ratio of surface to volume for nanoparticles, the interphase play a predominant role in nanocomposites. Silicone rubber composites filled with three kinds of nano silica were prepared and the effect of filler contents on the dielectric properties were investigated. The composites presented higher values of relative permittivity compared to pure silicone rubber as long the filler content increased. Based in a power-law relation to calculate the permittivity of composites which consider a factor for the particle shape, values for the interphase thickness and its value at different filler loads, were calculated. Values between 14 to 19 nm were estimated for the thickness of the interphase in the silica/silicone rubber systems and permittivities in the range of 7 to 23 were found for the interphase for compositions in the range of 2 to 10 vol%. From these values, some predictions for the interphase permittivity at higher filler concentrations were estimated.

## 1. INTRODUCTION

Polymeric insulating materials with nano-fillers homogeneously dispersed are called nanodielectric composites or simply nanocomposites [1]. These materials present favorable changes in their electrical, mechanical and thermal properties compared to conventionally used microcomposites and unfilled polymers [2, 3]. The principal reason for these changes in properties is related to the plurality of interfaces introduced through the use of nanomaterials due to as the particulate size reduces, the specific surface area becomes very large indeed. The interfacial area leads to a significant volume fraction of polymer surrounding the particle that has properties different from the bulk polymer (interaction zone) with a thickness on the order of one molecular radius of gyration (~5 to ~20 nm) [4]. A typical property of the bulk will be lost gradually as the particle shrinks in size and the interface influence more [7] as is shown in Figure 1.

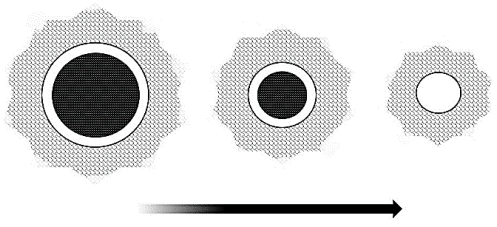

**Figure 1.** Interface properties become increasingly dominant as the particle size is reduced [7].

The role of the physics and chemistry at the interface may determine the behavior of the composite. This is very important since it means, in effect, that a truly new material is being created which differs from its constituents [5, 8, 9].

### *1.1 Interphase theory*

The volume of a composite $V_C$, can be expressed by the sum of the volumes of the matrix $V_M$, filler $V_F$ and the so-called the interphase volume $V_I$ as in Eq. (1). If it is divided by $V_C$ we obtain the relationship between the volume fractions of each component (Eq. (2)) [10]:

$$V_C = V_F + V_I + V_M \quad (1)$$

$$1 = \phi_F + \phi_I + \phi_M \quad (2)$$

where $\phi_F$, $\phi_I$ and $\phi_M$ are the volume fractions of filler, interphase and matrix respectively. Since $\phi_I$ must be zero when $\phi_F$ is zero or when $\phi_M$ is zero, it is expected the existence of a interphase volume constant $K_0$ given as

$$\phi_I = K_0 \phi_F \phi_M \quad (3)$$

$$\phi_M = \frac{1-\phi_F}{1+K_0\phi_F} \quad (4)$$

In Figure 2 are represented the variations in the interphase and matrix volume fractions respectively, depending on the changes in the volume fraction of the filler according Eq. (3) and Eq. (4). Small values of $K_0$

generate low quantities of interphase and a high volume of matrix. This could mean that the fillers have low specific surface area, big size, agglomeration and/or a thin interphase thickness due to a weak molecular link between filler and matrix. This could happen if one phase is hydrophilic and the other hydrophobic.

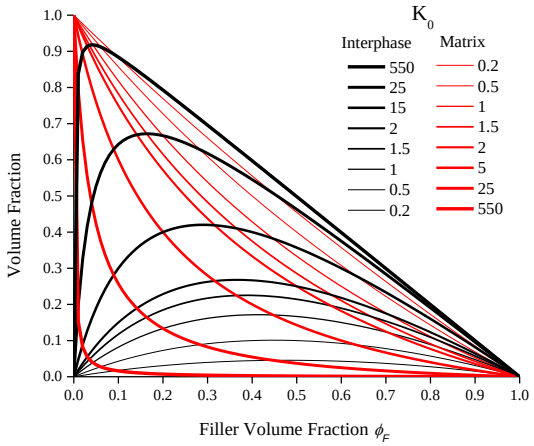


**Figure 2.** The interphase and matrix volume fractions as predicted by Eq. (3) and Eq. (4).

Higher $K_0$ values originate abrupt changes in the interphase and matrix volumes with just a little quantity of filler. This could be due to a very high specific surface area characteristic of well dispersed nanofillers and/or due to the formation of a very thick interphase, indicative of good affinity between filler and matrix, creating strong and long links among them.

Equations (3) and (4) represent ideal cases where the filler eventually can completely fill the volume where the composite is confined which just can be achieved through a kind of perfect stacking of fillers with shapes that allows them to be ordered without leaving gaps. Nevertheless, if all the fillers have the same size and spherical shape, the maximum volume fraction of fillers in the composite will be 74.1% determined by the ABAB structure [11] as in Figure 3.

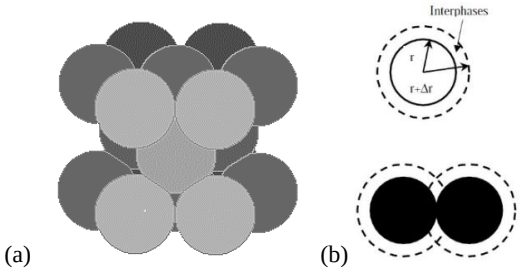


**Figure 3.** (a)The ABAB structure given the maximum filler volume fraction in a composite. (b) The interphase shell thickness $\Delta r$ around the filler of radius $r$ [10].

Hence, the interphase volume for the ABAB structure and its correspondent interphase volume fraction can be calculated according Eq. (5a) and Eq. (5b)

$$V_I = \frac{\frac{4\pi N}{3}[((r+\Delta r)^3 - r^3) - f6(3(r+\Delta r)-\Delta r)\Delta r^2]}{r^3} \quad (5a)$$

$$\phi_I = \frac{\frac{4\pi \phi_F}{3}[((r+\Delta r)^3 - r^3) - f6(3(r+\Delta r)-\Delta r)\Delta r^2]}{r^3} \quad (5b)$$

where $r$ is the filler radius, $\Delta r$ is the thickness of the interphase and $f$ ($0 \leq f \leq 1$) is the interphase overlap probability which arises from the proximity of the individual filler particles [4, 10]. The value of $f$ is normalized to obtain the maximum overlapping at 74.1% of filler volume fraction. According previous works [10, 12, 13] if the filler specific surface area $S_F$ is known, the interphase volume fraction $\phi_I$ for any random shape and distribution of filler particles with mass density $\rho_F$ may be obtained using the following Eq. 6 [4]:

$$\phi_I = (1-f)(S_F \cdot \Delta r) \cdot \rho_F \cdot \phi_F \quad (6)$$

where

$$f = \left(\frac{6\phi_F}{\pi}\right)^3 \quad (7)$$

Thereby, a detailed study of the changes' trend of the filler, matrix and interphase volumes, could yield information about the properties of the fillers incorporated to the matrix: quality of their dispersion, thickness of the interphase and even the strength of the linkage among phases.

### *1.2 Effective permittivity of nanocomposites*

Theories and models have been proposed attempting to describe interfaces and the properties that nanofilled composites exhibit as a result. Those models support the idea that an interface is formed around each nanoparticle generating a layer of partially "immobilized" polymer [20-22]. Power-law relationships are quite often used in dielectric modeling of two-component composite systems. For a composite comprised of 3 components: filler, interphase and matrix, the power law mixtures model may be generalized as Eq (8).

$$\varepsilon_C^\beta = \phi_F \varepsilon_F^\beta + \phi \varepsilon_I^\beta + \phi_M \varepsilon_M^\beta \quad (8)$$

where $\varepsilon_C$, $\varepsilon_F$, $\varepsilon_I$ and $\varepsilon_M$ are the complex dielectric permittivity of the composite, filler, interphase and matrix respectively. The dimensionless parameter $\beta$ represents the shape and orientation of the filler particles within the bulk composite. For a sphere this relationship reduces to 1/3 as predicted by Landau, Lifshitz and Looyenga [4, 23]. Empirical bounds that limit the range of permittivity predictions were established long ago by Weiner [24]. These bounds give the widest possible

range of permittivity predictions for two-component composite systems [26, 27]. The upper and lower Wiener bounds for a three-phase system are stated in Eq. (9a) and Eq. (9b) respectively:

$$\varepsilon_C = \phi_I \varepsilon_I - \phi_F \varepsilon_F - (1 - \phi_I - \phi_F)\varepsilon_M \quad \text{Eq. (9a)}$$

$$\frac{1}{\varepsilon_C} = \frac{\phi_I}{\varepsilon_I} + \frac{\phi_F}{\varepsilon_F} + \frac{1-\phi_I-\phi_F}{\varepsilon_M} \quad \text{Eq. (9b)}$$

Using the aforementioned equations, in this work the effective composite permittivity of silica/silicone rubber was modeled and a range of reasonable values for the interphase thickness and its permittivity were extracted.

## 2. EXPERIMENTAL

### *2.1 Materials*

Composites were prepared by dispersing nano silica particles ($SiO_2$) in two-part silicone rubber RTV615 (viscosity of 43 poises, $\varepsilon$=2.7 and $\rho$=1.8x10$^{15}$ $\Omega$·cm). The characteristics of the silica powders used during this work are listed in Table 1:

| Filler (Fumed Silica) | Average particle size (nm) | Specific surface area ($m^2/g$, BET) |
|---|---|---|
| Aerosil R202* | 14 | 100 ± 20 |
| Aerosil R812** | 7 | 260 ± 30 |
| Aerosil R8200** | 12 | 160 ± 25 |

**Table 1.** Fumed silica used as nanofillers [1]

### *2.2 Use of electrospinning as a dispersion method*

Ideally, a nanocomposite should be free of filler agglomerates but that is most often not easily achieved. Conventional mechanical mixing using high shear mixer (HS) or ultrasonic mixing cannot effectively break apart nanoparticles due to their high surface energies and the large Van der Waals forces between nanoscaled fillers.

Electrospinning (ES) is a straightforward process typically used to produce continuous nanofibres in diameters ranging from submicrons down to nanometers. This method is based in electrostatic forces to stretch the charged jet of polymer solution causing a tiny stream of solution to eject from the high voltage spinneret. When the jet flies away from the high voltage tip towards the grounded collector, it bends into a complex path and becomes further stretched and thinned in the large ratios. The advantage of this method is the diminution of filler agglomerates and the inexistence of chemical additives in the final composite because nanofillers are separated just by electrical forces [28-30].

### *2.3 Sample preparation*

The selected concentrations of silica fillers were 2, 4 and 8 vol% (3.8, 7.6 and 14.6 wt% respectively). The nanosilica was mixed with ethanol using an overhead stirrer to wet the nanofillers. Later, this solution was electrospun and mixed with RTV615-A at a constant flow rate to obtain the desired concentration of the nanofillers in the compound. RTV615-B was mixed into the collected electrospun polymer dispersion and the final mixture was again mechanically stirred and then poured into metallic moulds to be pressed and cured at 3300 Psi and 135 °C during 10 min. This method which is based in electrospinning and vulcanization in hot press conditions is named ES-HP. After these treatments the cured samples exhibited inexistence of air bubbles inside.

## 3. RESULTS AND DISCUSSION

### *3.1 Scanning Electron Microscopy (SEM) Images*

A scanning electron microscope (SEM) LEO FESEM 1530 was used to examine the degree of dispersion of the nanosilica in the RTV615 silicone rubber matrix. The samples for SEM observation were prepared by taking the cross-sections of nanocomposites. They were cut into small pieces through the cryo-cut method which consists in freezing the samples using liquid nitrogen. When the samples were solid enough, they were beaten, some pieces were recuperated and their flattest fractured surfaces identified in order to be observed, then they were sputter-coated with a thin gold layer. In Figures (4a) to (4c), the SEM corresponds to the samples made by the ES-HP method for samples containing R202, R812 and R8200 silica respectively. It is evident from the images that the samples show a reduced filler agglomeration and a homogenous filler dispersion.

### *3.2 Permittivity of Composites*

An insulation diagnostic analyzer IDAX 300 (Megger) was used to measure the capacitance and dissipation factor (tan $\delta$) of the nanocomposites under a range of frequencies from 0.5 mHz to 2 MHz. To corroborate these data, an E4980A LCP meter (Agilent) was used to measure the capacitance using a non-contact method in order to minimize errors due to irregularities in the samples' surfaces.

[1] * Fumed silica treated with PDMS (Polydimethylsiloxane) groups on the surface, ** Fumed silica treated with HMDS (Hexamethyldisilazane) groups on the surface.

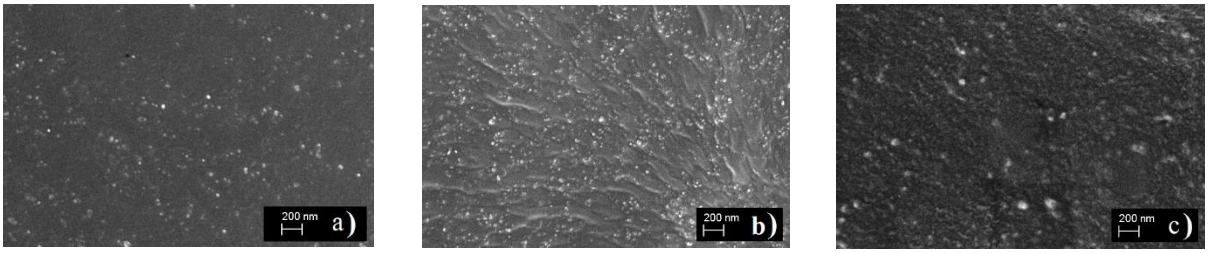


**Figure 4.** Cross-sectional morphology of silicone rubber nanocomposites with (a) 4 vol% R202 nanosilica and (b) 4 vol% R812 nanosilica and (c) 8 vol% R8200 nanosilica obtained by the ES-HP method.

The first instrument requires the calculation of the permittivity through the Eq. (11), the second apparatus offers the results calculated automatically.

$$\varepsilon_C = \frac{C \cdot d}{\varepsilon_0 \cdot A} \qquad (11)$$

Here $C$ is the capacitance of the sample, $d$ its thickness, $A$ is the contact area with the electrodes and $\varepsilon_0$ is the vacuum permittivity. Figure (5a) shows the increase in the permittivity for nanocomposites elaborated with R812 silica by using the ES-HP method. For R202 and R8200 powders, the increase in permittivity was higher just for the 2 vol% concentration as is shown in Figure (5b), for others concentrations the permittivity decreased.

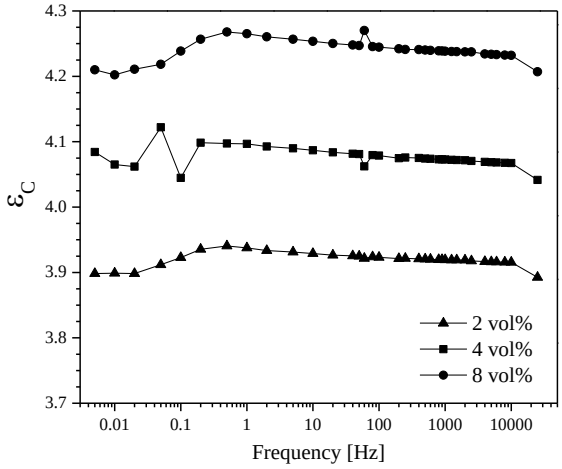


**Figure 5a.** Relative permittivity of the composites elaborated with R812 nanosilica at 2 vol%, 4 vol% and 8 vol%.

In both figures the relative permittivity shows a dip at about 60 kHz attributable to dielectric relaxation at this frequency. The dip gradually disappears with increase in filler content [31]. For the R812 fillers the relative permittivity of the composites was increased with increased filler concentrations. This result also can reconfirm the evidence that the ethanol solvent totally disappears from the electrospun samples during the evaporation stage as it effect does not alter the final composites. Figure 6 shows the permittivity and *tan* $\delta$ of R812 nanocomposites at 1 kHz. It is clear that $\varepsilon_C$ and *tan* $\delta$ increases with increasing filler content. As the filler loading increases, the connectivity between filler particles and dipole–dipole interaction increases, which can also lead to an increase in the relative permittivity [31].

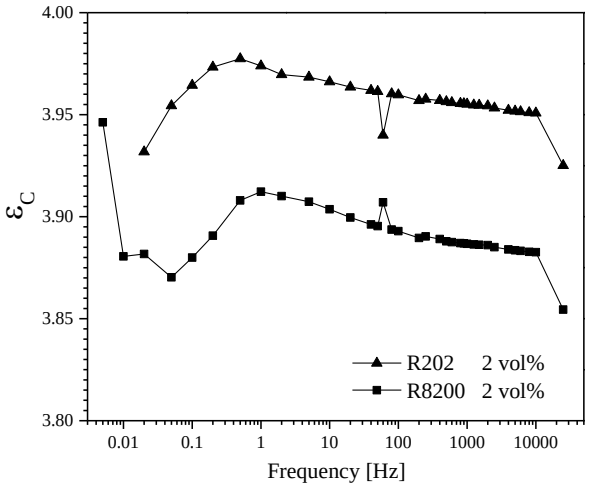


**Figure 5b.** Increments in relative permittivity of composites elaborated with R202 and R8200 nanosilica were observed for 2 vol% concentration.

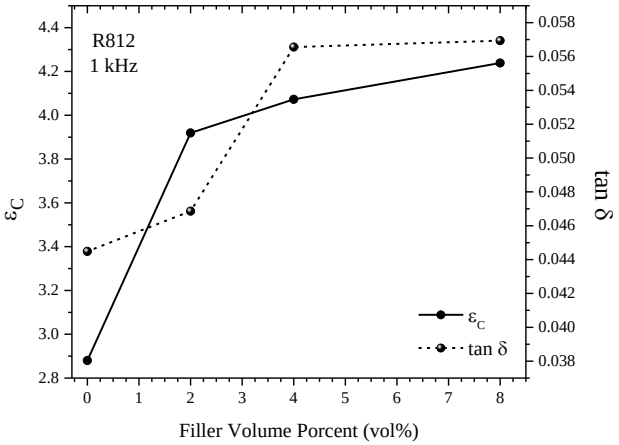


**Figure 6.** Variation of relative permittivity and dissipation factor of R812/silicone rubber nanocomposites at 1kHz.

## 4. MODEL PREDICTIONS

### *4.1 Modeling of the electrical properties of the interphase*

The interphase power-law model predicts a non-linearity in the effective dielectric constant and dielectric loss of the composites as a function of filler volume loading. This effect is shown in Figures (7a) to (7c), in which the experimental and the modeled effective dielectric constant at 1 kHz of the nanocomposites elaborated at different filler loads with R202, R812 and R8200 silica are displayed.

The trend of the permittivity behaviour was complemented with the theoretical upper and lower Wiener bounds for the three different batches of nanocomposites elaborated. It was necessary to change the value of the constant in Eq. (7) from 6 to 30 in order to achieve a good adjustment among the theory and the experimental data in the range of 0 to 10% of filler concentration. The values adjusted to fit the theoretical curves with the experimental data in order to obtain the trends in Figure 7 are listed in Table 2.

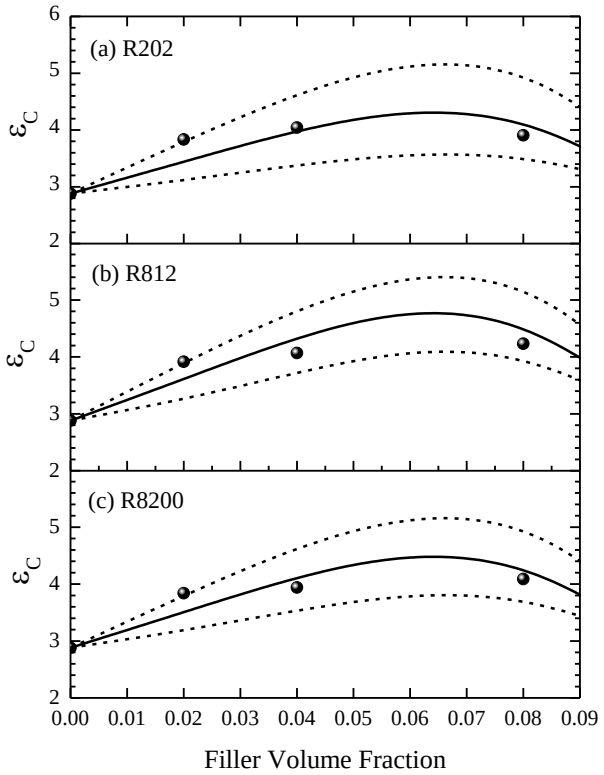


**Figure 7.** Predicted curves at 10 kHz for the relative permittivity of silicone rubber composites made with (a) R202, (b) R812 and (c) R8200 nano silica. Circular dots are the experimental values. The solid line represents the theoretical $\varepsilon_C$ and the dotted lines represent the upper and lower Wiener bounds.

These values can be considered a first insight to elucidate the properties of the interphase in these nanocomposite systems. They fit into the ranges predicted by other authors [1-4]. Considering the experimental values and the central trend for the relative permittivity of the composites in Figure 7, it is possible to find a theoretical trend for the interphase permittivity along other higher compositions that experimentally result difficult to obtain. In Figure 8 the values for $\varepsilon_I$ tend to decrease as the fraction of filler increases because the filler properties became more dominant and the volume of interphase decreases.

**Estimated properties of the interphase and fillers**

| Composite | $\varepsilon_I$ | $\Delta r$ (nm) | $S_F$ ($m^2/g$) |
|---|---|---|---|
| R202/RTV615 | $16 \pm 7$ | 19 | 120 |
| R812/RTV615 | $10 \pm 3$ | 13.9 | 290 |
| R8200/RTV615 | $11 \pm 4$ | 17 | 185 |

**Table 2.** Material characteristics of model polymer composite.

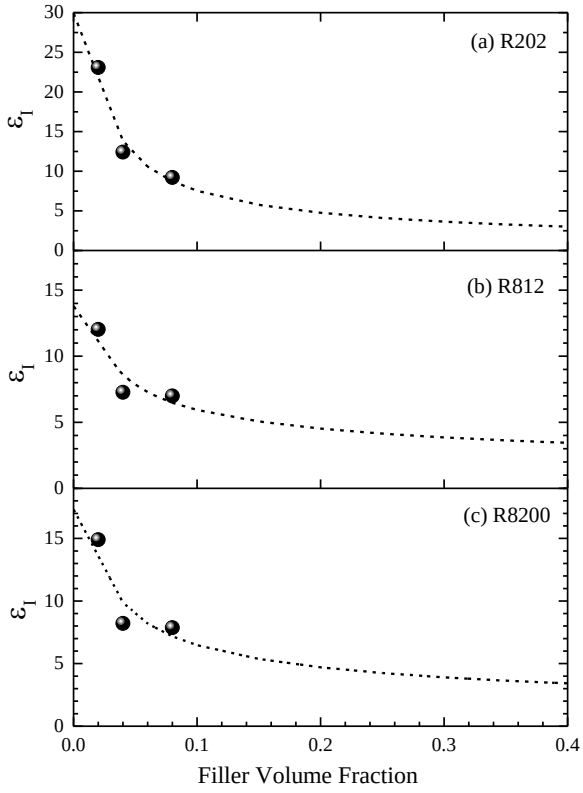


**Figure 8.** Predicted curves at 10 kHz for the relative permittivity of the interphase of silicone rubber composites made with (a) R202, (b) R812 and (c) R8200 nano silica. Circular dots represent the values obtained through experimental measurements and the dotted lines represent the theoretical $\varepsilon_I$ trend for the relativity permittivity of the interphase in these systems.

## 5. CONCLUSIONS

Trends in the composite material's effective permittivity as a function of filler volume fraction, interphase permittivity, interphase thickness as well as filler surface area were calculated. From this work, it is clear that the effect of the interphase region on the effective permittivity of nanocomposites can be significant. Furthermore, the effect of the interphase region on the effective permittivity of the composite system allows to obtain estimated values for other properties, as thickness and the specific surface area of the dispersed fillers in each composite. The extension of these estimated values for the interphase to calculate other physical, electrical or thermal characteristics of the composite systems is anticipated.

## ACKNOWLEDGEMENTS

The financial support from NSERC Canada. M. Paredes-Olguín is recipient of a post-doctoral fellowship by the Secretaría de Ciencia, Tecnología e Innovación del Distrito Federal (SECITI, Mexico City).

## REFERENCES

[1] T. Tanaka, M. Kozako, N. Fuse and Y. Ohki, "Proposal of a multi-core model for polymer nanocomposite dielectrics," *Dielectrics and Electrical Insulation, IEEE Transactions On,* vol. 12, pp. 669-681, 2005.

[2] J. Seiler and J. Kindersberger, "Insight into the Interphase in Polymer Nanocomposites," *IEEE Trans. Dielectr. Electr. Insul.,* vol. 21, pp. 537-547, APR 2014, 2014.

[3] M. Ezzat, N. A. Sabiha and M. Izzularab, "Accurate model for computing dielectric constant of dielectric nanocomposites," *Appl Nanosci,* vol. 4, pp. 331-338, 27 February 2013, 2014.

[4] M. Todd and F. Shi, *Dielectric Characteristics of Complex Composite Systems Containing Interphase Regions.* 2004.

[5] T. J. Lewis, "Interfaces are the dominant feature of dielectrics at the nanometric level," *Dielectrics and Electrical Insulation, IEEE Transactions On,* vol. 11, pp. 739-753, 2004.

[6] J. K. Nelson, *Overview of Nanodielectrics: Insulating Materials of the Future.* 2007.

[7] M. F. Fréchette, A. Vijh, M. L. Trudeau, D. Fabiani, L. Utracki, S. Gubanski, A. Sami, E. David, J. Kindersberger, C. Laurent, C. Reed, P. Morshuis, T. Andritsch, R. Kochetov, A. Krivda, A. Vaughan, J. Fothergill, S. Dodd, J. Castellon, F. Guastavino and H. Alamdari, "Nanodielectrics: A "universal" panacea for solving all electrical insulation problems?" in *Solid Dielectrics (ICSD), 2010 10th IEEE International Conference On,* 2010, pp. 1-3.

[8] M. Roy, J. K. Nelson, R. K. MacCrone, L. S. Schadler, C. W. Reed, R. Keefe and W. Zenger, "Polymer nanocomposite dielectrics - The role of the interface," *IEEE Trans. Dielectr. Electr. Insul.,* vol. 12, pp. 629-643, AUG 2005, 2005.

[9] Vo, H.T., Todd, M., Shi, F.G., Shapiro, A.A., Edwards,M., "Towards model-based engineering of underfill materials: CTE modeling," *Microelectron. J.,* vol. 32, pp. 331-338, 2001.

[10] H. T. Vo and F. G. Shi, "Towards model-based engineering of optoelectronic packaging materials: dielectric constant modeling," *Microelectron. J.,* vol. 33, pp. 409-415, 5/6, 2002.

[11] M. G. Todd and F. G. Shi, "Validation of a novel dielectric constant simulation model and the determination of its physical parameters," *Microelectron. J.,* vol. 33, pp. 627-632, AUG 2002, 2002.

[12] M. G. Todd and F. G. Shi, "Characterizing the interphase dielectric constant of polymer composite materials: Effect of chemical coupling agents," *J. Appl. Phys.,* vol. 94, pp. 4551-4557, OCT 1 2003, 2003.

[13] D. Pitsa and M. G. Danikas, "Modeling relative permittivity and electrical treeing in polymer nanocomposites," *Proceedings of the 2013 Ieee International Conference on Solid Dielectrics (Icsd 2013), Vols 1 and 2,* pp. 832-835, 2013, 2013.

[14] C. S. Daily, W. Sun, M. R. Kessler, X. Tan and N. Bowler, "Modeling the Interphase of a Polymer-based Nanodielectric," *IEEE Trans. Dielectr. Electr. Insul.,* vol. 21, pp. 488-496, APR 2014, 2014.

[15] J. K. Nelson and J. C. Fothergill, "Internal charge behaviour of nanocomposites," *Nanotechnology,* vol. 15, pp. 586-595, MAY 2004, 2004.

[16] K. K. Karkkainen, A. H. Sihvola and K. I. Nikoskinen, "Effective permittivity of mixtures: Numerical validation by the FDTD method," *IEEE Trans. Geosci. Remote Sens.,* vol. 38, pp. 1303-1308, MAY 2000, 2000.

[17] O. Wiener, "Zur theorie der Refraktionskonstanten," *Berichteu-Bie Verhandlungen Koniglich-Sachsischen Gesellschaft Wissenschaften Leipzig,* pp. 256-277, 1910.

[18] Z. Hashin and S. Shtrikman. A variational approach to the theory of the effective magnetic permeability of multiphase materials. *J. Appl. Phys. 33(10),* pp. 3125-3131. 1962.

[19] C. S. Daily, M. R. Kessler, Xaoli Tan and N. Bowler, "On the nanoparticle interphase," in *Electrical Insulation and Dielectric Phenomena (CEIDP), 2012 Annual Report Conference On,* 2012, pp. 507-510.

[20] M. G. Todd and F. G. Shi, "Complex permittivity of composite systems: A comprehensive interphase approach," *IEEE Trans. Dielectr. Electr. Insul.,* vol. 12, pp. 601-611, JUN 2005, 2005.

[21] Shanshan Bian, S. H. Jayaram and E. A. Cherney, "Use of electrospinning to disperse nanosilica into silicone rubber," in *Electrical Insulation and Dielectric Phenomena (CEIDP), 2010 Annual Report Conference On,* 2010, pp. 1-4.

[22] S. Bian, S. Jayaram and E. A. Cherney, "Electrospinning as a New Method of Preparing Nanofilled Silicone Rubber Composites," *IEEE Trans. Dielectr. Electr. Insul.,* vol. 19, pp. 777-785, JUN, 2012.

[23] A. H. El-Hag, L. C. Simon, S. H. Jayaram and E. A. Cherney, "Erosion resistance of nano-filled silicone rubber," *IEEE Trans. Dielectr. Electr. Insul.,* vol. 13, pp. 122-128, FEB 2006, 2006.

[24] L. K. Namitha, J. Chameswary, S. Ananthakumar and M. T. Sebastian, "Effect of micro- and nano-fillers on the properties of silicone rubber-alumina flexible microwave substrate," *Ceram. Int.,* vol. 39, pp. 7077-7087, AUG 2013, 2013.